

AD-A068 630

ARMY ELECTRONICS RESEARCH AND DEVELOPMENT COMMAND FO--ETC F/G 9/1
STATIC AND DYNAMIC FREQUENCY - TEMPERATURE CHARACTERISTICS OF Q--ETC(U)
APR 79 A BALLATO

UNCLASSIFIED

DELET-TR-79-8

NL

1 OF 1
AD
A068630



END
DATE
FILMED
6-79
DDC



LEVEL

AD

RESEARCH AND DEVELOPMENT TECHNICAL REPORT

DELET-TR-79-8

STATIC AND DYNAMIC FREQUENCY - TEMPERATURE CHARACTERISTICS OF QUARTZ VIBRATORS

AD A 068630

DDC
RECEIVED
MAY 15 1979
C

Arthur Ballato
ELECTRONICS TECHNOLOGY & DEVICES LABORATORY

April 1979

DISTRIBUTION STATEMENT
Approved for public release;
distribution unlimited.

DDC FILE COPY

ERADCOM

US ARMY ELECTRONICS RESEARCH & DEVELOPMENT COMMAND
FORT MONMOUTH, NEW JERSEY 07703

79 05 14 029

NOTICES

Disclaimers

The citation of trade names and names of manufacturers in this report is not to be construed as official Government indorsement or approval of commercial products or services referenced herein.

Disposition

Destroy this report when it is no longer needed. Do not return it to the originator.

UNCLASSIFIED

SECURITY CLASSIFICATION OF THIS PAGE (When Data Entered)

REPORT DOCUMENTATION PAGE		READ INSTRUCTIONS BEFORE COMPLETING FORM
1. REPORT NUMBER 14 DELET-TR-79-8	2. GOVT ACCESSION NO.	3. RESEARCH CATALOG NUMBER 9 Research and development
4. TITLE (and Subtitle) 6 STATIC AND DYNAMIC FREQUENCY - TEMPERATURE CHARACTERISTICS OF QUARTZ VIBRATORS.	5. TYPE OF REPORT & PERIOD COVERED Technical Report.	
7. AUTHOR(s) 10 Arthur Ballato	8. CONTRACT OR GRANT NUMBER(s) 17 09	
9. PERFORMING ORGANIZATION NAME AND ADDRESS US Army Electronics Technology & Devices Laboratory (ERADCOM) Ft. Monmouth, N.J. 07703 DELET-MM	10. PROGRAM ELEMENT, PROJECT, TASK AREA & WORK UNIT NUMBERS 16 1L1 61101 A91A 09 478	
11. CONTROLLING OFFICE NAME AND ADDRESS US Army Electronics Research & Development Command Fort Monmouth, N.J. 07703 DELET-MM	12. REPORT DATE 11 Apr 79	
14. MONITORING AGENCY NAME & ADDRESS (if different from Controlling Office) 12 33 p.	13. NUMBER OF PAGES 28	
15. SECURITY CLASS. (of this report) UNCLASSIFIED		15a. DECLASSIFICATION/DOWNGRADING SCHEDULE
16. DISTRIBUTION STATEMENT (of this Report) Approved for public release; distribution unlimited.		
17. DISTRIBUTION STATEMENT (of the abstract entered in Block 20, if different from Report)		
18. SUPPLEMENTARY NOTES		
19. KEY WORDS (Continue on reverse side if necessary and identify by block number) Crystal resonators AT-cut quartz Crystal oscillators Quartz crystals Piezoelectric crystals Frequency control Piezoelectric vibrators Frequency-Temperature Characteristics		
20. ABSTRACT (Continue on reverse side if necessary and identify by block number) The frequency-temperature (f-T) behavior of a crystal resonator depends upon temperature, and its spatial and temporal gradients. For quasi-isothermal changes, the static f-T curve can be used to determine frequency shifts that occur. The frequency then depends upon the parameters of the static f-T curve, the temperature range over which the oven cycles, and upon the oven setting point. The maximum frequency excursion has been computed for the AT and SC cuts of quartz in terms of these parameters, as function of orientation angle. When oven cyclings, or other temperature perturbations occur at rates (con't)		

DD FORM 1 JAN 73 1473

EDITION OF 1 NOV 65 IS OBSOLETE

UNCLASSIFIED

SECURITY CLASSIFICATION OF THIS PAGE (When Data Entered)

410 698

LM

UNCLASSIFIED

SECURITY CLASSIFICATION OF THIS PAGE (When Data Entered)

too rapid to be considered quasi-isothermal, additional non-negligible components of frequency shift are introduced. This effect is quantified by means of a simple model which is capable of predicting thermal transient effects for AT cuts. Simulations, using the model, disclose that sinusoidal temperature variations with periods of hours can lead to frequency instabilities much larger than would be expected using the static f-T curve. This effect should be greatly diminished in the vicinity of the SC cut. ↖

ACCESSION for	
NTIS	White Section <input checked="" type="checkbox"/>
DOC	Buff Section <input type="checkbox"/>
UNANNOUNCED	<input type="checkbox"/>
JUSTIFICATION	
BY	
DISTRIBUTION/AVAILABILITY CODES	
Dist.	SP. CIAL
A	

UNCLASSIFIED

SECURITY CLASSIFICATION OF THIS PAGE (When Data Entered)

CONTENTS

INTRODUCTION	1
STATIC BEHAVIOR	2
DYNAMIC EFFECTS	2
EXPERIMENTAL RESULTS	15
SINUSOIDAL VARIATIONS	16
CONCLUSIONS	25
REFERENCES	26

FIGURES:

1. Definition of oven characteristics on resonator curve	3
2. Normalized frequency excursion for AT-cut quartz	4
3. Normalized frequency excursion for SC-cut quartz	8
4. Simulation of hysteresis from sinusoidal temperature cycling	17
5. Simulation of frequency hysteresis. Ten kelvin sweep	18
6. Hysteresis loops offset from upper turnover point	19
7. Elliptical orbits for sweep range of 5 millikelvins	20
8. Elliptical orbits for sweep ranges of 0.5 and 1 millikelvin	21
9. Elliptical orbits for sweep range of 1 millikelvin	23

TABLES:

1. Frequency deviations for AT-cut quartz, with $\Delta\theta = 5'$ and transient effects omitted	5
2. Frequency deviations for AT-cut quartz, with $\Delta\theta = 0.5'$ and transient effects omitted	6
3. Values of K_1 and K_2 in equation (3) for AT-cut quartz and $\Delta\theta$ in minutes of arc	7
4. Frequency deviations for SC-cut quartz, with $\Delta\theta = 5'$	9
5. Frequency deviations for SC-cut quartz, with $\Delta\phi = 5'$	10

6.	Frequency deviations for SC-cut quartz, with $\Delta\theta = 0.5'$. . .	11
7.	Frequency deviations for SC-cut quartz, with $\Delta\phi = 0.5'$. . .	12
8.	Values of K_1 and K_2 in equation (3) for SC-cut quartz and $\Delta\theta$ in minutes of arc	13
9.	Values of K_1 and K_2 in equation (3) for SC-cut quartz and $\Delta\phi$ in minutes of arc	14
10.	Frequency deviations due to dynamic thermal behavior of AT-cut resonator of reference 20	24

INTRODUCTION

In their sixty years, quartz resonators have shown themselves capable of dramatic improvements in frequency stability: on the average, one order of magnitude per decade. Because of a long history compared with other solid state devices, it is easy to look upon this component as the product of a mature technology, and to presume that the leveling-off plateau has been reached; that the last bit of stability has been, or shortly is to be, wrung out of the venerable vibrator.

Such a conclusion would be entirely wrong. Prospects are exceedingly good that the near-term future will see a further hundred-fold improvement in the stability of high precision oscillators, brought about by using doubly rotated quartz resonators of special orientations. This development fortunately coincides with stringent frequency control requirements newly imposed by the latest generations of communication systems and systems for navigation and position location.^{1-38*}

In order to identify an important present contribution to frequency instability, and to separate out its effects, it is convenient to discuss first the static frequency-temperature (f-T) characteristic of a quartz resonator¹. Static f-T curves are of interest in their own right in connection with crystals operating without ovens over broad temperature ranges, such as in temperature compensated crystal oscillators². Maximum frequency deviations, obtained from the static f-T curves, are shown to be simply represented in normalized form for such applications. They are subsequently used for comparison with the dynamic behavior of resonators.

For crystal resonators subjected to wide temperature variations, the angle of cut is ordinarily chosen to minimize the frequency excursions over the entire temperature range. High precision oscillators, on the other hand, utilize resonators maintained within an oven system that closely regulates the thermal environment. In this latter case it is important to know how the unavoidable oven instabilities affect the resonator frequency, and how the oven parameters interact with the f-T curve as a function of crystal cut.

Use of the static f-T curve, in conjunction with the known characteristics of commercial ovens, leads to the conclusion that frequency stabilities orders of magnitude better than those observed, ought to be possible with AT-cut resonators. The discrepancy is mainly due to the neglect of the dynamic f-T behavior of the crystal. By making use of various types of dynamic f-T data from the literature, a phenomenological parameter can be extracted that satisfactorily explains the effects found in practice. When applied to simulations of oven cycling, it shows the dominance of dynamic effects in high stability situations when AT cuts are used.

At the SC cut, the parameter linking dynamic thermal behavior to frequency becomes zero for thickness-directed temperature gradients, and for this doubly rotated quartz cut, the f-T behavior predicted from the static curve is capable of being realized.

In the first part of this technical report the static f-T behavior of AT and SC cuts is examined. The dynamic behavior of resonators is considered in

* See list of references beginning on page 26.

the second portion.

STATIC BEHAVIOR

For most types of quartz resonators, the frequency-temperature behavior takes the form of the cubic curve depicted in Figure 1. When the resonator is operated in an oven there will be, in general, an oven offset error Δ that measures the amount by which the oven setting point misses the desired reference point where the first order temperature coefficient vanishes. In addition, the oven will have a cycling range, $\pm \Delta T_0$, about the setting point, as seen in Figure 1. As the oven cycles, the frequency will vary, and in the case shown, the maximum frequency excursion will be from the reference point to the frequency at the point $\Delta + \Delta T_0$. As Δ and ΔT_0 are allowed to vary, the maximum frequency excursion will of course vary, and will be a function of Δ , ΔT_0 , and the shape of the cubic curve. The cubic varies with the angle of cut. For the AT and SC cuts of orientations $(YX\ell)\theta \approx 35.2^\circ$; $(YX\omega\ell)\theta \approx 21.9^\circ / \theta \approx 33.9^\circ$, the reference angle is taken as that for which turnover temperatures coincide with the inflection temperature. In terms of deviations $\Delta\theta$ from this angle, the maximum frequency excursions are shown for AT cut quartz in Figure 2. The angle difference is in minutes of arc, and the ordinate is the quantity

$$\sigma = |\Delta f/f| \text{ max.} / \{(\Delta T_0)^2 \cdot (1 + |\rho|)^2\}. \quad (1)$$

Rho is defined as $\rho = \Delta/\Delta T_0 = 2 \cdot \text{offset/cycle range.} \quad (2)$

For $|\rho| \leq 1$, a single curve suffices. The curves may be closely approximated by the relation

$$\sigma \approx (K_1 + K_2 \Delta\theta) \cdot (\Delta\theta)^{1/2} \quad (3)$$

where σ is the ordinate expressed in (1) and K_1, K_2 are simple functions of $|\rho|$ for a given cut. Tables 1 and 2 provide values of $|\Delta f/f| \text{ max.}$ for AT-cut quartz, for $\Delta\theta = 5$ and 0.5 minutes of arc, respectively. Table 3 gives values of K_1 and K_2 for a wide range of values of ρ , for the AT cut.

The doubly rotated SC cut of orientation $(YX\omega\ell)\theta \approx 21.9^\circ / \theta \approx + 33.9^\circ$ has two angles to vary. Figure 3 gives the variation in σ versus $\Delta\theta$. Tables 4 and 5 present values of $|\Delta f/f| \text{ max.}$ for $\Delta\theta$ and $\Delta\theta = 5'$, respectively, while Tables 6 and 7 are for $\Delta\theta$ and $\Delta\theta = 0.5'$, also respectively. Tables 8 and 9 give values of K_1 and K_2 , as function of ρ , for the SC cut; Table 8 for $\Delta\theta$ and Table 9 for $\Delta\theta$.

With reference to Table 2, one sees that an AT-cut operated in a good oven with a stability of a few millikelvins should produce frequency stabilities in the order 10^{-13} to 10^{-14} . This in fact is far from the actual values obtained.

DYNAMIC EFFECTS

That the resonance frequency of a crystal vibrator depends on temperature-rate and gradient effects, as well as temperature itself has been known for some time³⁻²⁶. Experimental evidence exists in a number of forms. Bistline¹³ showed that the f-T cubic curve appeared to exhibit cut angles differing in $\Delta\theta$ by several minutes of arc for different temperature sweep rates. Kusters²⁰ showed how the upper turning point of an AT-cut shifts in frequency with temperature rate. In both cases the temperature-time graphs were ramps, so that

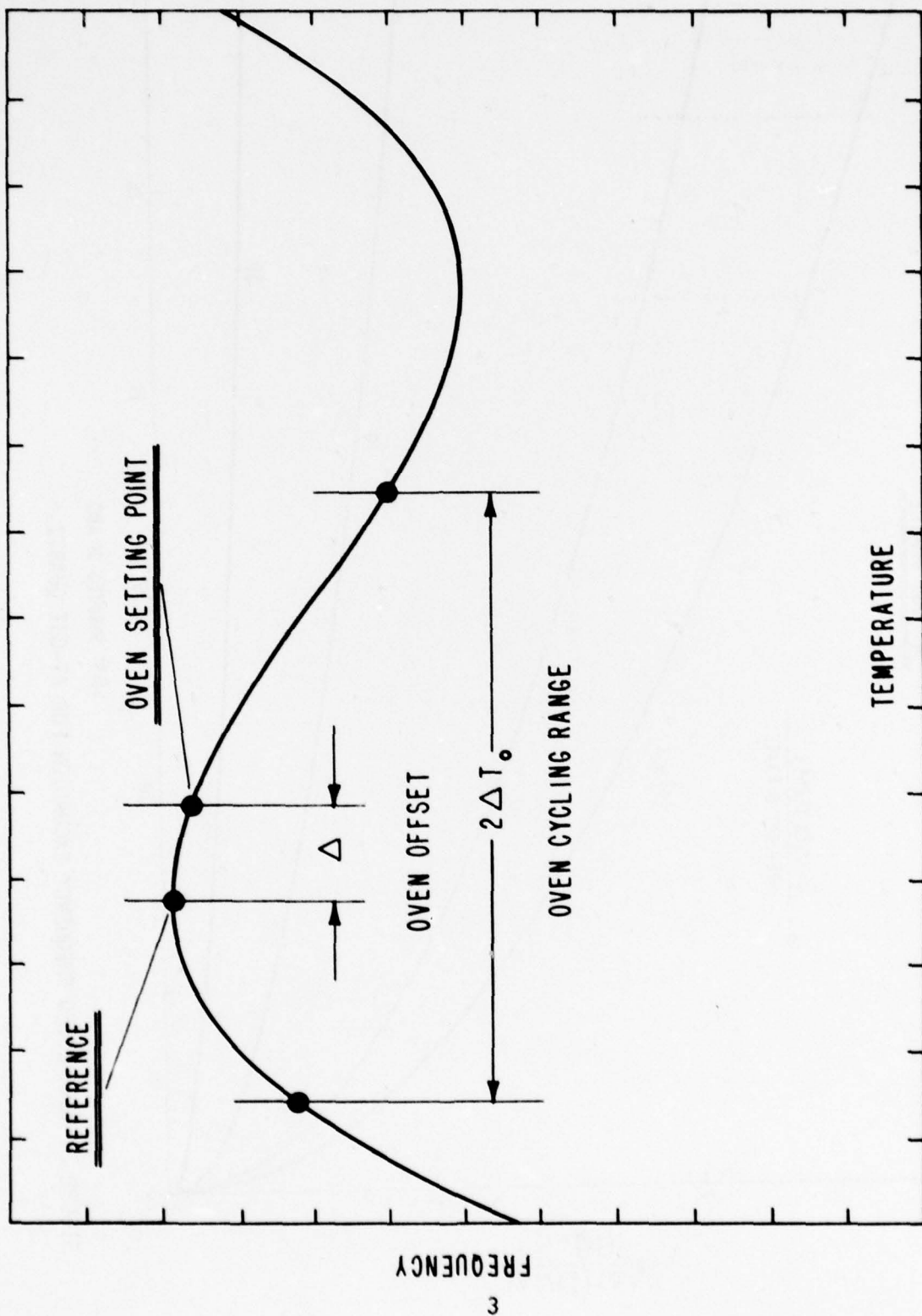


FIGURE 1. DEFINITION OF OVEN CHARACTERISTICS ON RESONATOR CURVE.

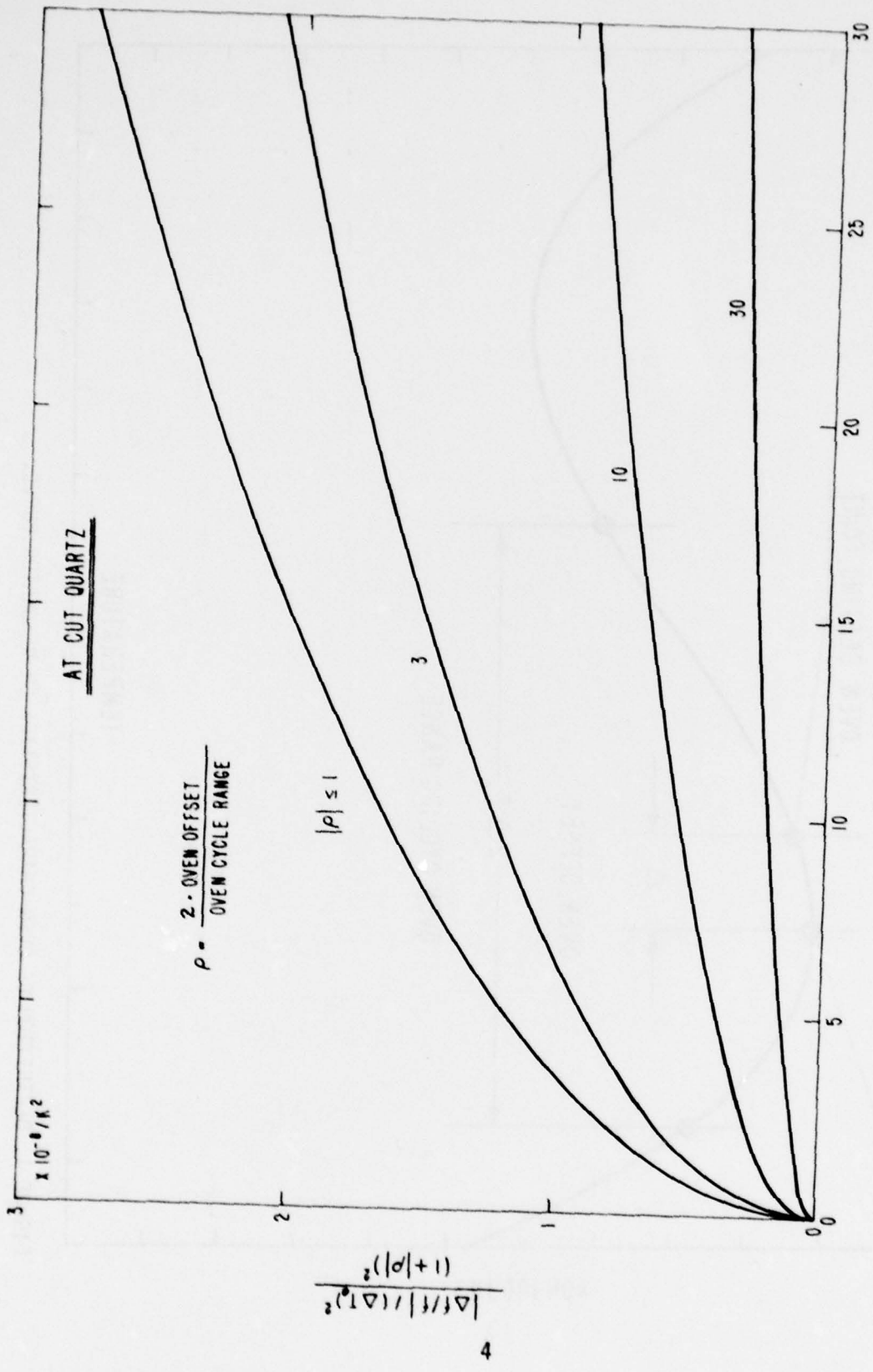


FIGURE 2. NORMALIZED FREQUENCY EXCURSION FOR AT-CUT QUARTZ.

TABLE 1. FREQUENCY DEVIATIONS FOR AT-CUT QUARTZ, WITH $\Delta\theta=5'$ AND TRANSIENT EFFECTS OMITTED.

$\Delta\theta = 5'$		OVEN CYCLING RANGE (K)			
		1	0.1	0.01	0.001
OVEN OFFSET (K)	1	4.6×10^{-8}	4.6×10^{-9}	4.6×10^{-10}	4.6×10^{-11}
	0.1	1.4×10^{-8}	4.7×10^{-10}	4.7×10^{-11}	4.7×10^{-12}
	0.01	1.2×10^{-8}	1.4×10^{-10}	4.7×10^{-12}	4.7×10^{-13}
	0.001	1.2×10^{-8}	1.2×10^{-10}	1.4×10^{-12}	4.7×10^{-14}
	0	1.2×10^{-8}	1.2×10^{-10}	1.2×10^{-12}	1.2×10^{-14}

TABLE 2. FREQUENCY DEVIATIONS FOR AT-CUT QUARTZ, WITH $\Delta\theta = 0.5'$ AND TRANSIENT EFFECTS OMITTED.

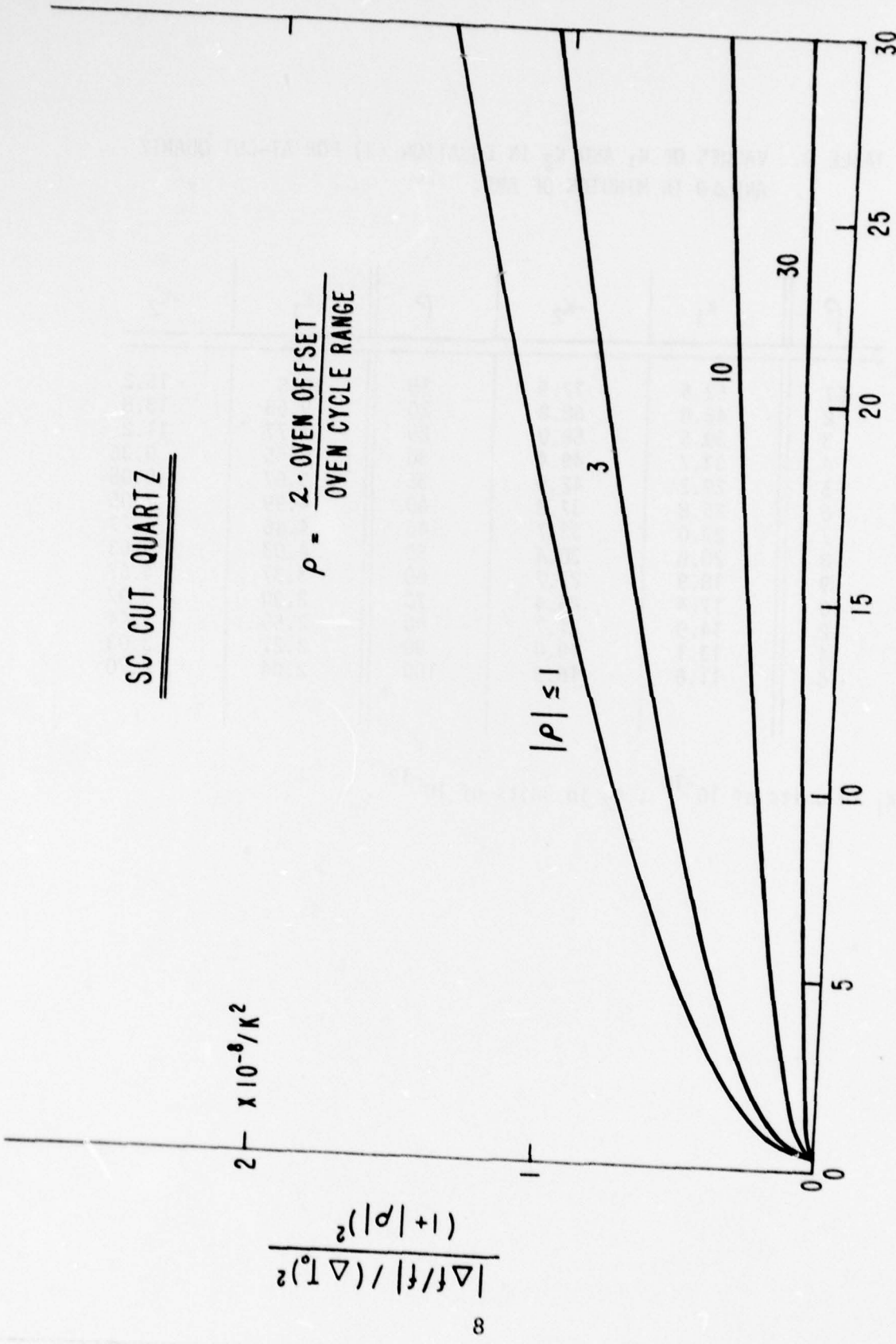
$\Delta\theta = .5'$	OVEN CYCLING RANGE (K)				
	1	0.1	0.01	0.001	
OVEN OFFSET (K)	1	1.4×10^{-8}	1.4×10^{-9}	1.4×10^{-10}	1.4×10^{-11}
	0.1	4.4×10^{-9}	1.5×10^{-10}	1.5×10^{-11}	1.5×10^{-12}
	0.01	3.8×10^{-9}	4.5×10^{-11}	1.5×10^{-12}	1.5×10^{-13}
	0.001	3.8×10^{-9}	3.8×10^{-11}	4.5×10^{-13}	1.5×10^{-14}
	0	3.8×10^{-9}	3.8×10^{-11}	3.7×10^{-13}	3.7×10^{-15}

TABLE 3. VALUES OF K_1 AND K_2 IN EQUATION (3) FOR AT-CUT QUARTZ AND $\Delta\theta$ IN MINUTES OF ARC.

ρ	K_1	$-K_2$	ρ	K_1	$-K_2$
≤ 1	52.6	77.5	18	10.5	15.2
2	46.8	68.8	20	9.53	13.8
3	39.5	58.0	25	7.77	11.2
4	33.7	49.4	30	6.55	9.36
5	29.2	42.9	35	5.67	8.05
6	25.8	37.8	40	4.99	7.05
7	23.0	33.7	45	4.46	6.27
8	20.8	30.4	50	4.03	5.63
9	18.9	27.7	60	3.37	4.67
10	17.4	25.4	70	2.90	3.97
12	14.9	21.7	80	2.55	3.44
14	13.1	19.0	90	2.27	3.03
16	11.6	16.9	100	2.04	2.70

K_1 in units of 10^{-10} ; K_2 in units of 10^{-13} .

SC CUT QUARTZ



$$\rho = \frac{2 \cdot \text{OVEN OFFSET}}{\text{OVEN CYCLE RANGE}}$$

$\Delta \theta$ MINUTES OF ARC

FIGURE 3. NORMALIZED FREQUENCY EXCURSION FOR SC-CUT QUARTZ.

TABLE 4. FREQUENCY DEVIATIONS FOR SC-CUT QUARTZ, WITH $\Delta\theta = 5'$.

$\Delta\theta = 5'$	OVEN CYCLING RANGE (K)			
	1	0.1	0.01	0.001
1	2.1×10^{-8}	2.1×10^{-9}	2.1×10^{-10}	2.1×10^{-11}
0.1	6.5×10^{-9}	2.2×10^{-10}	2.2×10^{-11}	2.2×10^{-12}
0.01	5.4×10^{-9}	6.5×10^{-11}	2.2×10^{-12}	2.2×10^{-13}
0.001	5.4×10^{-9}	5.5×10^{-11}	6.5×10^{-13}	2.2×10^{-14}
0	5.4×10^{-9}	5.4×10^{-11}	5.4×10^{-13}	5.4×10^{-15}

OVEN OFFSET (K)

TABLE 5. FREQUENCY DEVIATIONS FOR SC-CUT QUARTZ, WITH $\Delta\phi = 5'$.

$\Delta\phi = 5'$	OVEN CYCLING RANGE (K)			
	1	0.1	0.01	0.001
OVEN OFFSET (K)	1	5.9×10^{-9}	6.0×10^{-11}	6.0×10^{-12}
	0.1	1.8×10^{-9}	6.3×10^{-11}	6.3×10^{-13}
	0.01	1.6×10^{-9}	1.9×10^{-11}	6.3×10^{-14}
	0.001	1.6×10^{-9}	1.6×10^{-11}	1.9×10^{-13}
	0	1.6×10^{-9}	1.6×10^{-11}	1.6×10^{-13}

TABLE 6. FREQUENCY DEVIATIONS FOR SC-CUT QUARTZ, WITH $\Delta\theta = 0.5'$.

$\Delta\theta = .5'$	OVEN CYCLING RANGE (K)				
	1	0.1	0.01	0.001	
OVEN OFFSET (K)	-	6.3×10^{-9}	6.4×10^{-10}	6.4×10^{-11}	6.4×10^{-12}
	0.1	2.0×10^{-9}	6.7×10^{-11}	6.7×10^{-12}	6.7×10^{-13}
	0.01	1.7×10^{-9}	2.0×10^{-11}	6.7×10^{-13}	6.7×10^{-14}
	0.001	1.7×10^{-9}	1.7×10^{-11}	2.0×10^{-13}	6.7×10^{-15}
	0	1.7×10^{-9}	1.7×10^{-11}	1.7×10^{-13}	1.7×10^{-15}

TABLE 7. FREQUENCY DEVIATIONS FOR SC-CUT QUARTZ, WITH $\Delta\phi=0.5'$.

$\Delta\phi = .5'$	OVEN CYCLING RANGE (K)				
	1	0.1	0.01	0.001	
OVEN OFFSET (K)	-	1.6×10^{-9}	1.7×10^{-10}	1.7×10^{-11}	1.7×10^{-12}
	0.1	5.4×10^{-10}	2.0×10^{-11}	2.0×10^{-12}	2.0×10^{-13}
	0.01	5.4×10^{-10}	6.0×10^{-12}	2.0×10^{-13}	2.0×10^{-14}
	0.001	5.5×10^{-10}	5.1×10^{-12}	6.1×10^{-14}	2.0×10^{-15}
	0	5.5×10^{-10}	5.1×10^{-12}	5.0×10^{-14}	5.0×10^{-16}

TABLE 8. VALUES OF K_1 AND K_2 IN EQUATION (3) FOR SC-CUT QUARTZ
AND $\Delta\theta$ IN MINUTES OF ARC.

ρ	K_1	$-K_2$	ρ	K_1	$-K_2$
≤ 1	34.5	86.0	18	6.87	17.0
2	30.7	76.4	20	6.25	15.4
3	25.9	64.4	25	5.09	12.5
4	22.1	54.9	30	4.30	10.5
5	19.2	47.6	35	3.72	9.10
6	16.9	42.0	40	3.27	7.99
7	15.1	37.5	45	2.92	7.12
8	13.6	33.8	50	2.64	6.42
9	12.4	30.8	60	2.21	5.35
10	11.4	28.3	70	1.90	4.58
12	9.79	24.3	80	1.67	3.99
14	8.58	21.2	90	1.49	3.54
16	7.63	18.9	100	1.34	3.17

K_1 in units of 10^{-10} ; K_2 in units of 10^{-13} .

TABLE 9. VALUES OF K_1 AND K_2 IN EQUATION (3) FOR SC-CUT QUARTZ
AND $\Delta\phi$ IN MINUTES OF ARC.

ρ	K_1	$+K_2$	ρ	K_1	$+K_2$
≤ 1	10.7	0.691	18	2.12	0.308
2	9.50	0.651	20	1.93	0.299
3	8.01	0.585	25	1.57	0.282
4	6.83	0.532	30	1.32	0.270
5	5.93	0.490	35	1.14	0.261
6	5.23	0.457	40	1.01	0.254
7	4.67	0.431	45	0.897	0.249
8	4.21	0.409	50	0.810	0.245
9	3.84	0.390	60	0.677	0.239
10	3.52	0.376	70	0.581	0.234
12	3.03	0.351	80	0.509	0.230
14	2.65	0.334	90	0.452	0.228
16	2.36	0.319	100	0.406	0.225

K_1 in units of 10^{-10} ; K_2 in units of 10^{-13} .

$\dot{T} = dT/dt$ is a constant. The influence of a "step function" of temperature on AT-cuts was shown by Warner^{7,11} and Munn¹⁴. For BT-cut and rotated-X-cut crystals²⁷, the frequency spike is reversed in sign. Based upon the observed effects, a number of models have been used to characterize thermal transient, or dynamic thermal, behavior of quartz resonators^{9,16,19,21,24}.

We propose here a simple model that explains the results of a variety of experiments. More careful experiments, coupled with a thorough analysis involving nonlinear elasticity theory are required to provide a firm foundation for understanding dynamic effects in resonators. It is hoped that the results presented here will stimulate such an approach to the problem. The traditional manner of expressing the static frequency-temperature behavior of quartz resonators is due to Bechmann²⁸:

$$\Delta f/f = a_0 \Delta T + b_0 \Delta T^2 + c_0 \Delta T^3. \quad (4)$$

In Eq. (4), $\Delta T = T - T_0$, where T is the present temperature, and T_0 is the specified reference temperature, often taken as 25°C, or as the inflection temperature, in which case b_0 equals zero.

The parameters a_0 , b_0 , and c_0 depend on material, cut, geometry, electroding, etc., but do not depend on time, for a given resonator design. Our assumption consists of the inclusion of the term $\tilde{a} \cdot \dot{T}$ in the expression for the effective first-order temperature coefficient $a(t)$, which now depends on time implicitly through the temporal behavior of the temperature:

$$\Delta f(t)/f = a(t) \cdot \Delta T(t) + b_0 \Delta T(t)^2 + c_0 \Delta T(t)^3, \quad (5)$$

with

$$a(t) = a_0 + \tilde{a} \cdot \dot{T}(t). \quad (6)$$

The quantity \tilde{a} is a function of the same entities as a_0 , b_0 , c_0 , as well as several others such as method of setting up thermal gradients (thickness gradient, azimuth-dependent lateral gradients), thermal conductivity of supports and electrodes, elasticity of, and stresses in, the electrodes, etc., but is a constant for a given design. It is treated simply as a phenomenological quantity to be evaluated separately for each crystal design. It is obvious that the assumption concerning $a(t)$ could be extended to the coefficients b_0 and c_0 , by introducing similar constants \tilde{b} and \tilde{c} ; the results are qualitatively the same, and they will be omitted here.

EXPERIMENTAL RESULTS

For the case of a ramp temperature-time profile, where \dot{T} is constant, $a(t)$ will reduce to a constant, different from a_0 . The f - T curve appears as if it had simply changed its apparent orientation angle θ . In the case of Bistline's graphs, the value of \tilde{a} required to account for the data is $+1.7 \times 10^{-7} \text{ s/K}^2$. This value is arrived at using the known quantity $da/d\theta = -5.08 \times 10^{-6}/\text{K, deg.}\theta$ for the AT cut^{2,23} to convert between changes in the coefficient "a" and the angle θ .

Applying the model to Kusters' curves²⁰, straightforward algebra yields the relation for the normalized frequency shift of the turning point

$$\delta = (T_\mu - T_0) \cdot \tilde{a} \cdot \dot{T}, \quad (7)$$

where T_μ is the upper turnover temperature and T_0 is the reference temperature.

Using the parameters of the AT-cut crystal discussed by Kusters²⁰, the value of $\tilde{\alpha}$, for the crystal used by him, is

$$\tilde{\alpha} = -2.27 \times 10^{-7} \text{ s/K}^2. \quad (8)$$

The Warner curves^{7,11,14} may be simulated closely by making the assumption that the thermal "step function" is of form $(1 - e^{-t/\tau})$, and involves a single system thermal time constant τ . The values of $\tilde{\alpha}$ are larger in magnitude than for the Bistline and Kusters experiments. The sign of $\tilde{\alpha}$ changes according to the electrode metallization pattern, being negative for thickness excitation and positive for electrodes with a gap for lateral excitation¹¹. It may be expected that other factors will influence the sign and size of $\tilde{\alpha}$, and that a proper choice of resonator and electrode design, electrode material(s) and method of deposition, will produce resonators with small $\tilde{\alpha}$ values. The possibility of controlling $\tilde{\alpha}$ by use of doubly rotated plates is discussed below.

The presence of a frequency spike, found by Warner⁷ in response to a thermal step function applied to an AT cut bulk wave resonator, has been recently verified for surface acoustic wave (SAW) resonators of ST-cut orientation by Parker²⁹.

SINUSOIDAL VARIATIONS

Based upon the simple model adopted it is possible to simulate the effect of sweeping the temperature in a sinusoidal manner. It is known that this leads experimentally to hysteresis effects. The result of a wide temperature range sweep is shown in Figure 4. The heavy line represents the static f-T curve. When the temperature is swept as $\sin \omega t$ by 60K about the 30°C point, the resulting curve exhibits an hysteresis that varies with the rate ω as shown. The effect is more pronounced at the upper turning point (UTP); this is due to the sign of $\tilde{\alpha}$. The orbits are counter-clockwise, also because of the sign of $\tilde{\alpha}$, at the UTP.

The general features of the curves in Figure 4, representing dynamic thermal cyclings, have been verified in the main by experiments performed by Hughes³⁰ using sinusoidal temperature cyclings. In particular, the much greater deviations at the UTP (implying a negative $\tilde{\alpha}$ in his experiment), compared with the lower turning point, were unequivocally established for the resonator examined.

Figure 5 shows the hysteresis effects expected for +10K excursions about the UTP. For a sweep with a 10-minute period the frequency change is roughly three times that expected on the basis of the static curve. In Figure 6 are shown hysteresis orbits for $\Delta T_0 = 5\text{K}$, offset from the UTP at T_μ by +5K and by -10K.

The frequency scale is magnified in Figure 7 to parts in 10^{-10} . For temperature deviations ΔT_0 of $+5 \times 10^{-3}\text{K}$, the static f-T curve is nearly a horizontal line, while the orbits for the dynamic frequency behavior are elliptical, with amplitudes greatly exceeding the static behavior when the period of the temperature cycle is shorter than about one hour. The constant $\tilde{\alpha}$ from Eq. (8) has been used in the computations. In Figure 8 the frequency scale has been further magnified to the 10^{-12} range, with a temperature scale in millikelvins about the UTP. Again is seen the dominance of the dynamic behavior

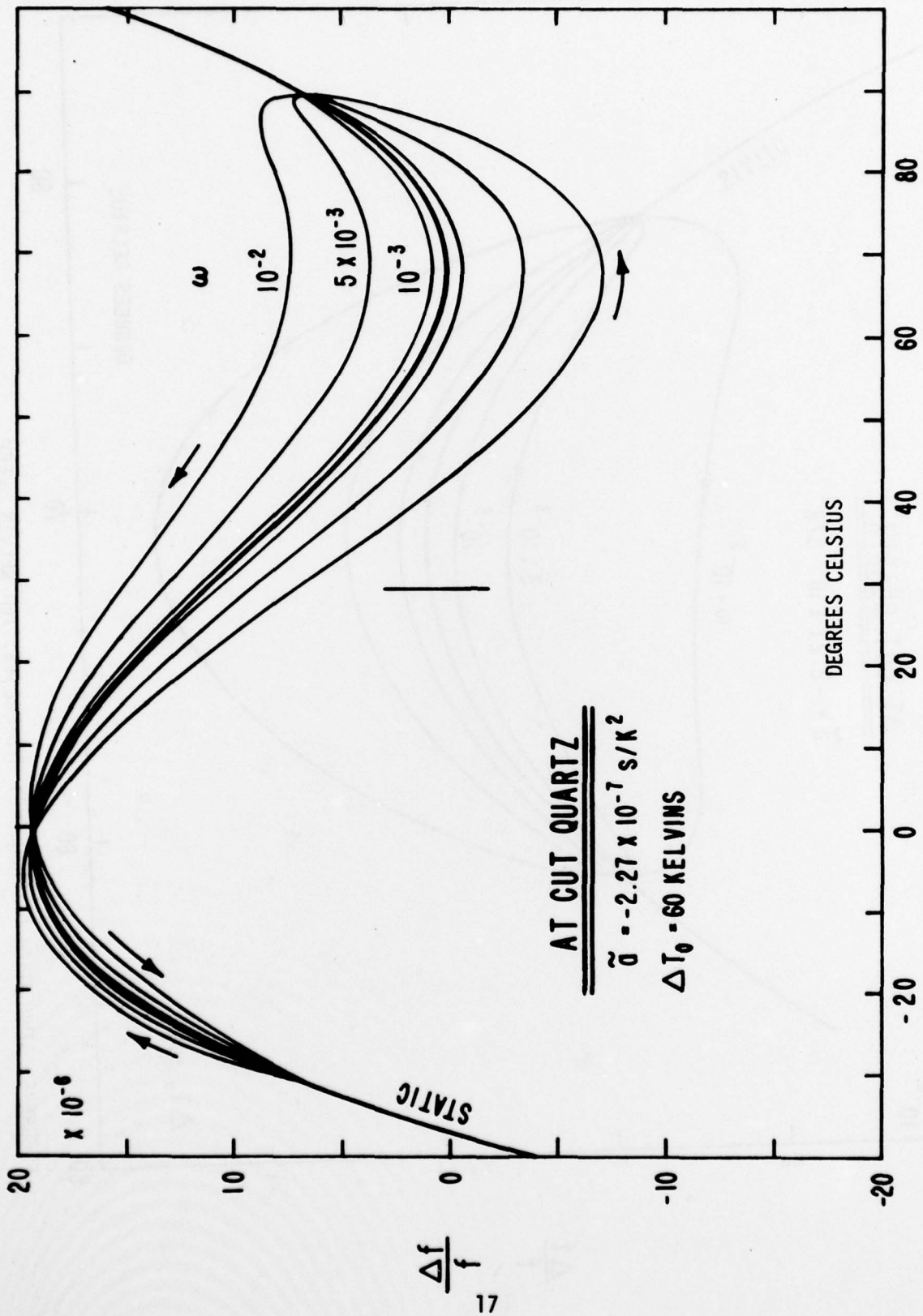


FIGURE 4. SIMULATION OF HYSTERESIS FROM SINUSOIDAL TEMPERATURE CYCLING.

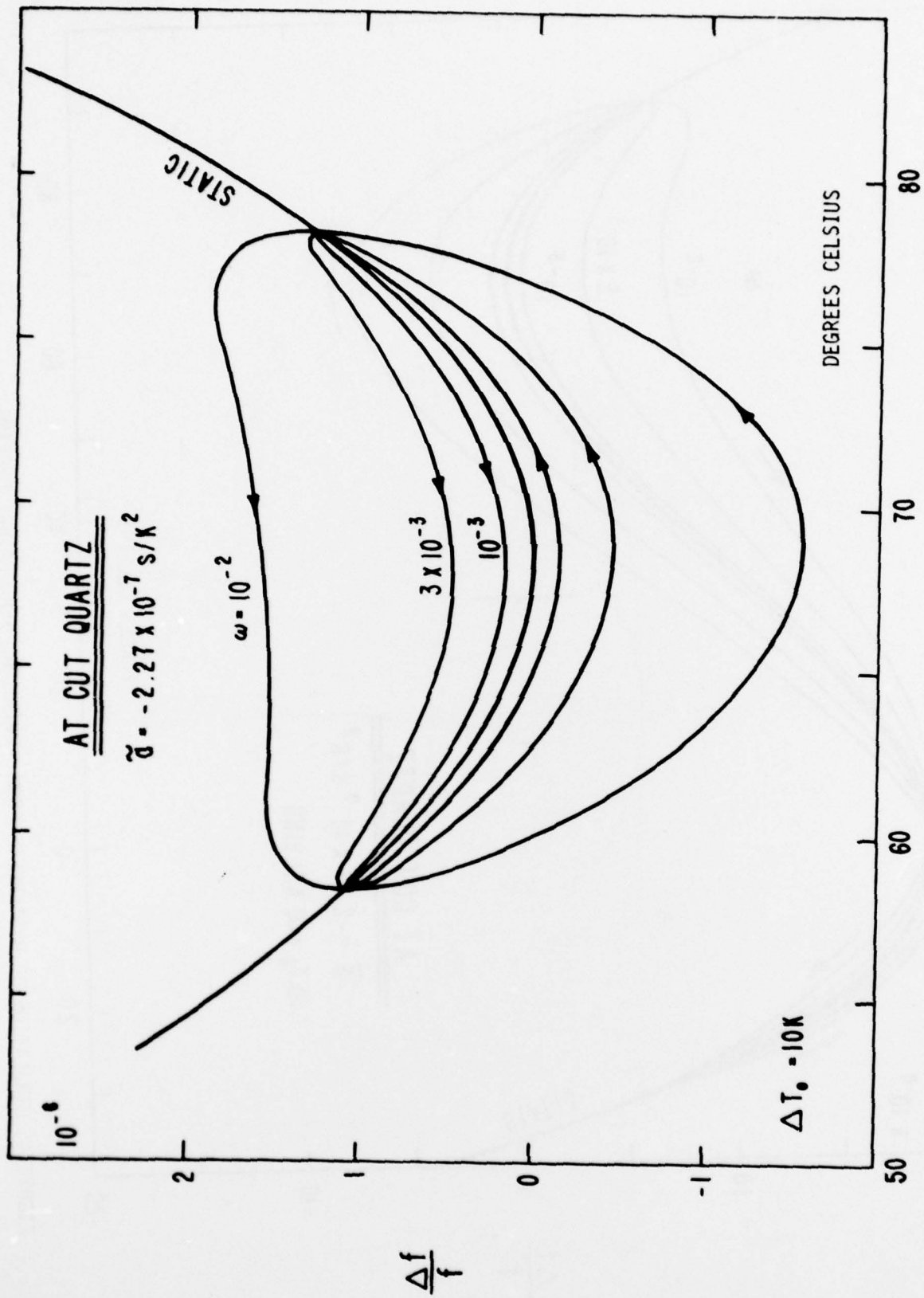


FIGURE 5. SIMULATION OF FREQUENCY HYSTERESIS. TEN KELVIN SWEEP.

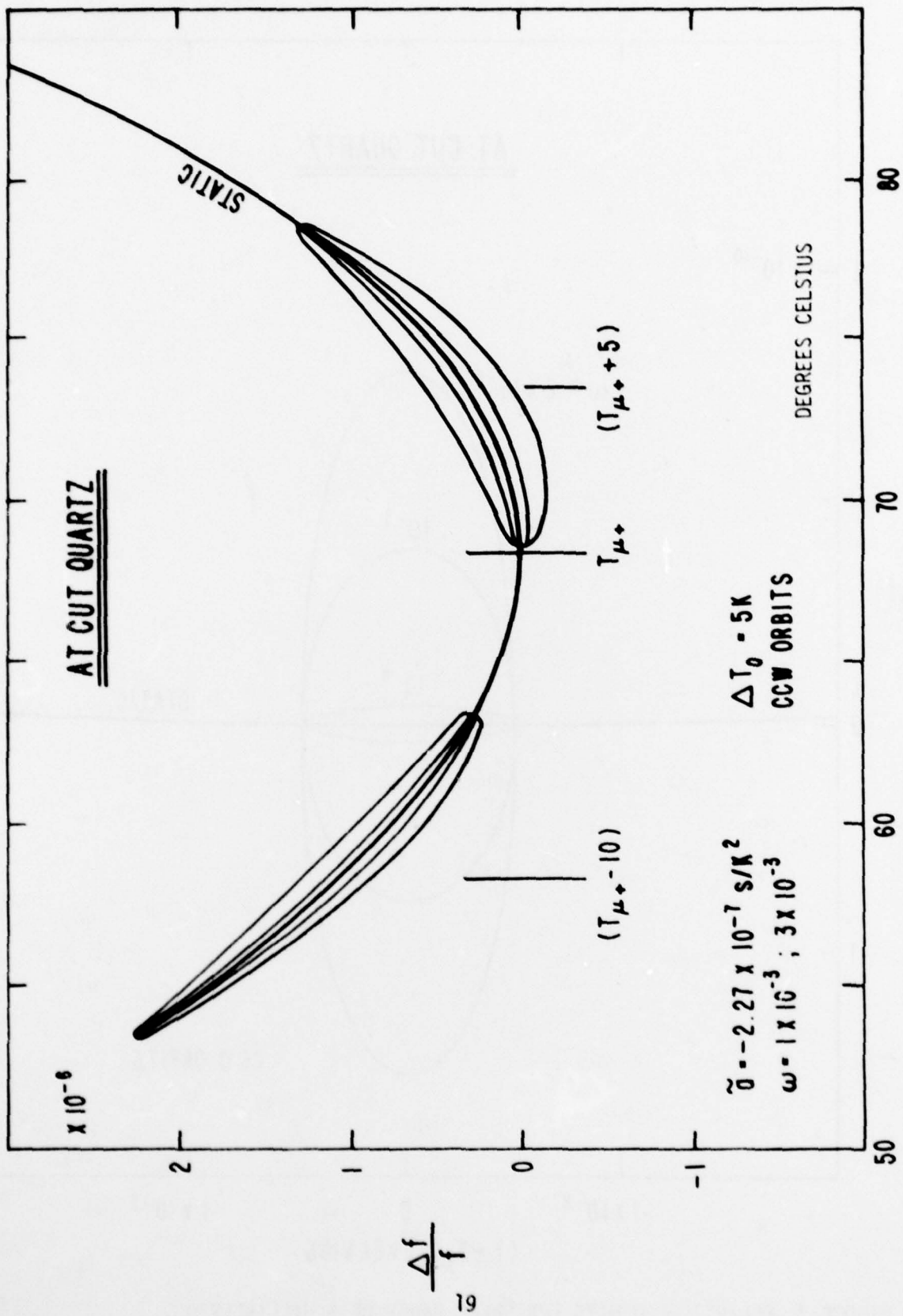


FIGURE 6. HYSTERESIS LOOPS OFFSET FROM UPPER TURNOVER POINT.

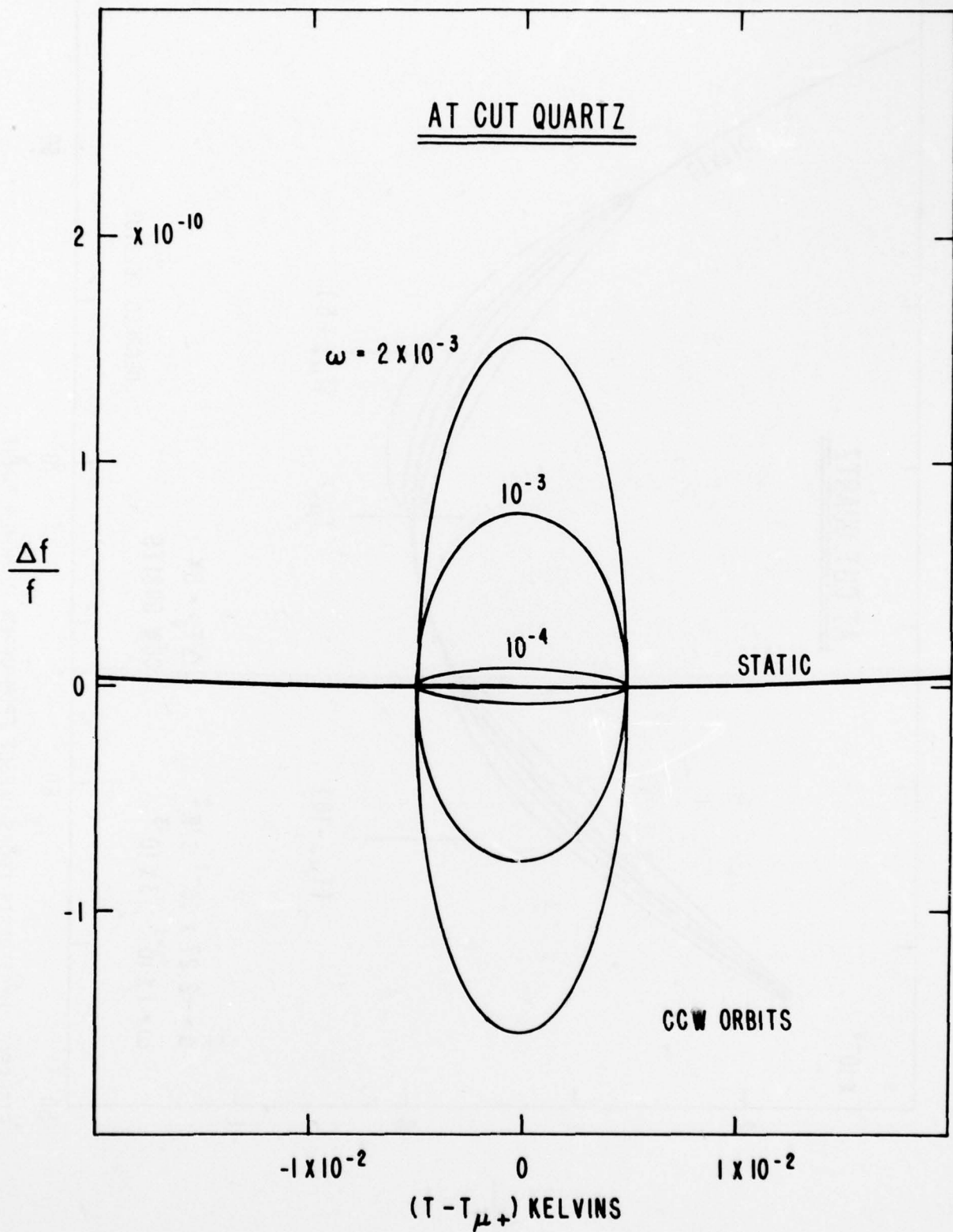


FIGURE 7. ELLIPTICAL ORBITS FOR SWEEP RANGE OF 5 MILLIKELVINS.

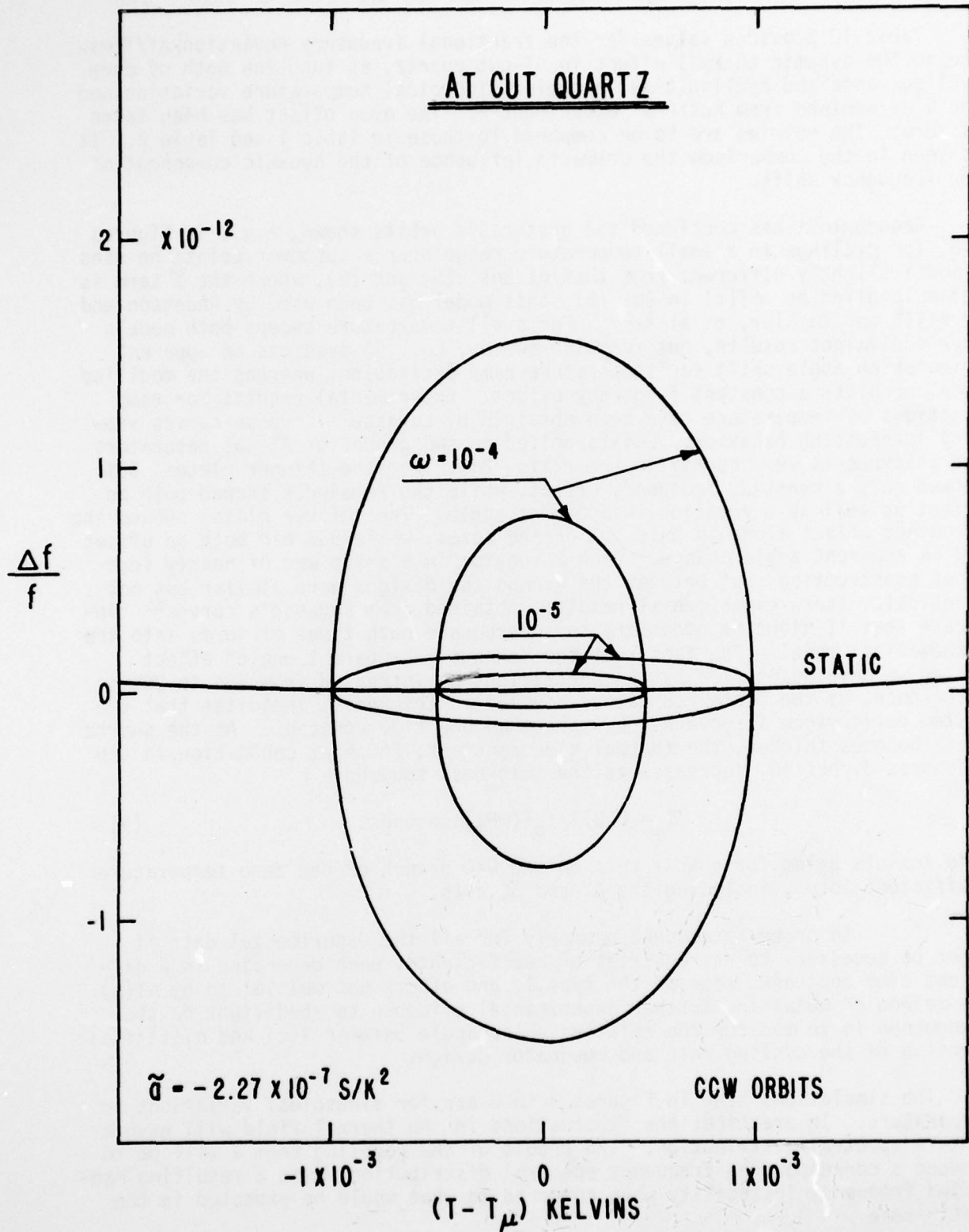


FIGURE 8. ELLIPTICAL ORBITS FOR SWEEP RANGES OF 0.5 AND 1 MILLIKELVIN.

compared to the static, even when the temperature variations take place over periods of the order of a day. Figure 9 shows the orbit for $\omega = 2 \times 10^{-4}$ also.

Table 10 provides values for the fractional frequency deviation $|\Delta f/f|_{\max}$ due to the dynamic thermal effect in AT-cut quartz, as function both of oven cycling range and cycling time, assuming sinusoidal temperature variation and the $\tilde{\alpha}$ determined from Kusters' experiment²⁰. The oven offset has been taken as zero. The entries are to be compared to those in Table 1 and Table 2. It is seen in the comparison the dramatic influence of the dynamic component of the frequency shift.

Gagnepain³¹ has confirmed the hysteresis orbits shown, e.g., in Figures 5-8, for cyclings in a small temperature range near a turnover point; he uses a model slightly different from that of Eqs. (5) and (6), where the $\tilde{\alpha}$ term is not multiplied by $\Delta T(t)$ in Eq. (5); this model has been used by Anderson and Merrill⁹ and Koehler, et al.^{21,24}. For small temperature sweeps both models give equivalent results, but for wide sweeps, Eq. (5) predicts an apparent orientation angle shift for temperature ramp excitation, whereas the modified model predicts a constant frequency offset. Experimental results for ramp functions of temperature have been obtained by Lagasse³², whose curves show very interesting behavior. Data supplied on two groups of AT-cut resonators had thicknesses very nearly in the ratio 2:1. For the thinner plates, 60% showed only a constant frequency offset, while the remainder showed both an offset as well as a rotation in apparent angle. The thicker plates showed the frequency offset alone in only 10% of the cases, while 90% had both an offset and an apparent angle change. Each resonator in a group was of nearly identical construction, but between the groups the designs were similar but not identical. These experimental results, obtained from Lagasse's curves³² indicate that it might be necessary to incorporate both types of terms into the mathematical model. The fact that the "change in apparent angle" effect (which we have quantified by the coefficient $\tilde{\alpha}$) increased from 40% to 90% in occurrence, as the plate resonators doubled in thickness, indicates that the system performance is governed by more than one time constant. As the quartz plate becomes thicker, the thermal time constant, for heat conduction in the thickness direction, increases as the thickness squared:

$$\tau = 0.271/f_0^2(\text{MHz}) \text{ seconds.} \quad (9)$$

This formula holds for quartz cuts on the $\theta > 0$ branch of the zero temperature coefficient locus, including the AT and SC cuts.

In order to account properly for all the experimental data it might be necessary to use a series of coefficients, each depending on a different time constant, some of the type $\tilde{\alpha}$, and others not multiplied by $\Delta T(t)$. One method of obtaining further experimental evidence to shed light on the phenomenon is to monitor the relative phase angle between $T(t)$ and $\Delta f(t)/f$ as function of the cycling rate and resonator design.

The simulations seen in Figures 4 to 8 are for sinusoidal variations in temperature. In practice, the fluctuations in the thermal field will have a certain spectral distribution. The result of the coupling term $\tilde{\alpha}$ will be to produce a corresponding frequency spectral distribution, with a resulting magnified frequency instability when compared to what would be expected in the static case.

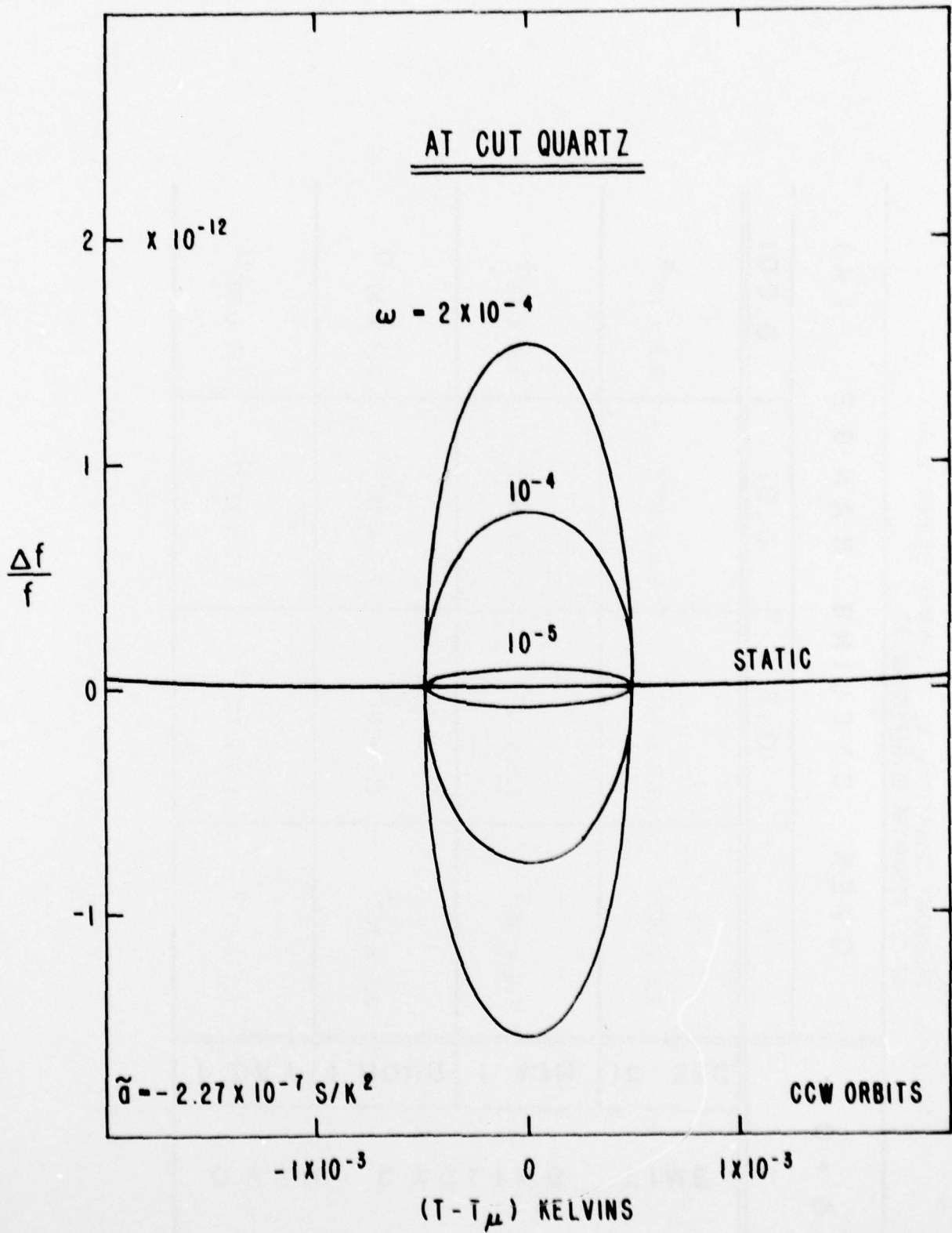


FIGURE 9. ELLIPTICAL ORBITS FOR SWEEP RANGE OF 1 MILLIKELVIN.

What are the prospects for reducing $\tilde{\alpha}$? Fortunately, it appears that by design even AT-cut resonators can be produced with smaller values of $\tilde{\alpha}$. However, by using doubly rotated crystals cut to orientations in the vicinity of the SC-cut the value of $\tilde{\alpha}$ can be reduced to a negligible value. These cuts are compensated for a variety of other effects as well^{23,33,34}. For rotated-X-cuts on the zero temperature coefficient locus³⁵ the approximate value for $\tilde{\alpha}$ is $+1.8 \times 10^{-7}$ s/K² for EerNisse's design. For a given vibrator design, a plot of $-\tilde{\alpha}$ versus θ along the upper zero temperature coefficient locus in quartz would look very much like Figure 3 in Reference 33; the derivative $\partial \tilde{\alpha} / \partial \theta$ is zero at the AT-cut, and reaches its maximum positive value at the rotated-X-cut.

The SC cut permits the possibility of a revolutionary change in the stabilities of crystal oscillators, particularly in the intermediate-to-long-term regimes. With the coefficient $\tilde{\alpha}$ reduced to a negligible level, and with state-of-the-art ovens in the millikelvin range, stabilities in the range 10^{-13} to 10^{-14} ought to be achievable. A stability of 6×10^{-14} for 128 second sampling times has recently been measured using an SC-cut crystal of special design, with an airgap fixture and special mountings^{36,37}. This stability also depended upon a special circuit configuration in addition to the SC-cut resonator³⁸. The ability to achieve medium-term stabilities on this order would make doubly rotated quartz resonators comparable to rubidium atomic frequency standards in precision applications. Medium precision stabilities will, in addition, be available for fast warmup oscillators, and represents a second important application area for these latest representatives of a long line of quartz vibrators.

CONCLUSIONS

The actual frequency instabilities observed in quartz crystal oscillators for medium- and high-precision applications are greater than can be accounted for by the static frequency-temperature characteristic of the vibrator and the noise characteristics of the active devices and ancillary circuitry. One mechanism contributing to the instability is the dynamic f-T coupling. This report has used available experimental data with a simple mathematical model to explore some of the consequences of the dynamic effect on the characteristics of the crystal resonance frequency.

Doubly rotated quartz resonators that are compensated for the dynamic thermal effect offer promise in the near-term future of making available very small, light weight, and cheap oscillators with stabilities approaching those of rubidium frequency standards.

REFERENCES*

1. A. Ballato and J.R. Vig, "Static and Dynamic Frequency-Temperature Behavior of Singly and Doubly Rotated, Oven Controlled Quartz Resonators", Proc. 32nd AFCS, May - June 1978, pp. 180-188.
2. A. Ballato, "Frequency-Temperature-Load Capacitance Behavior of Resonators for TCXO Application", IEEE Trans. Sonics Ultrason., Vol. SU-25, July 1978, pp. 185-191.
3. J.S. Lukesh and D.G. McCaa, "An Anomalous Thermal Effect in Quartz Oscillator-Plates", Am. Mineral., Vol. 32, March - April 1947, pp. 137-140.
4. V.E. Bottom, "Note on the Anomalous Thermal Effect in Quartz Oscillator Plates", Am. Mineral., Vol. 32, September-October 1947, pp. 590-591.
5. I.E. Fair, "Design Data on Crystal Controlled Oscillators", Appendix II in Information Bulletin on Quartz Crystal Units, ASES 52-9. Fort Monmouth, NJ, August 1952, 103 pp.
6. A.W. Warner, "Ultra-Precise Quartz Crystal Frequency Standards", IRE Trans. Instrumentation, Vol. I-7, December 1958, pp. 185-188.
7. A.W. Warner and D.L. White, "An Ultra-Precise Standard of Frequency", Eleventh Interim Report on Contract DA 36-039 SC-73078 to US Army Signal R&D Laboratory, Fort Monmouth, NJ, July 1959, 42 pp.
8. A.W. Warner, "Design and Performance of Ultraprecise 2.5-mc Quartz Crystal Units", Bell Syst. Tech. J., Vol. 39, September 1960, pp. 1193-1217.
9. T.C. Anderson and F.G. Merrill, "Crystal-Controlled Primary Frequency Standards: Latest Advances for Long-Term Stability", IRE Trans. Instrumentation, Vol. I-9, September 1960, pp. 136-140.
10. W.J. Spencer and W.L. Smith, "Precision Crystal Frequency Standards", Proc. 15th AFCS, May-June 1961, pp. 139-155.
11. A.W. Warner, "Use of Parallel-Field Excitation in the Design of Quartz Crystal Units", Proc 17th AFCS, May 1963, pp. 248-266.
12. W.L. Smith and W.J. Spencer, "Quartz Crystal Thermometer for Measuring Temperature Deviations in the 10^{-3} to 10^{-6} °C Range", Rev. Sci. Instr., Vol. 34, March 1963, pp. 268-270.
13. G. Bistline, Jr., "Temperature Testing Tight Tolerance Crystal Units", Proc. 17th AFCS, May 1963, pp. 314-315.
14. R.J. Munn, "Warm-up Characteristics of Oscillators Employing 3. M.C. Fundamental Crystals in HC-27/U Enclosures", Proc. 19th AFCS, April 1965, pp. 658-668.

*AFCS= Annual Frequency Control Symposium, US Army Electronics R&D Command, Fort Monmouth, N.J. 07703.

15. H.F. Pustarfi, "An Improved 5 MHz Reference Oscillator for Time and Frequency Standard Applications", IEEE Trans. Instrum. and Meas., Vol. IM-15, December 1966, pp. 196-202.
16. L.E. Schnurr, "The Transient Thermal Characteristics of Quartz Resonators and Their Relation to Temperature-Frequency Curve Distortion", Proc. 21st AFCS, April 1967, pp. 200-210.
17. E.F. Hartman and J.C. King, "Calculation of Transient Thermal Imbalance within Crystal Units Following Exposure to Pulse Irradiation", Proc. 27th AFCS, June 1973, pp. 124-127.
18. R. Holland, "Nonuniformly Heated Anisotropic Plates: I. Mechanical Distortion and Relaxation", IEEE Trans. Sonics Ultrason., Vol. SU-21, July 1974, pp. 171-178.
19. R. Holland, "Nonuniformly Heated Anisotropic Plates: II. Frequency Transients in AT and BT Quartz Plates", Proc. IEEE Ultrason. Symp., November 1974, pp. 592-598.
20. J.A. Kusters, "Transient Thermal Compensation for Quartz Resonators", IEEE Trans. Sonics Ultrason., Vol. SU-23, July 1976, pp. 273-276.
21. D.R. Koehler, T.J. Young, and R.A. Adams, "Radiation Induced Transient Thermal Effects in 5 MHz AT-cut Resonators", Proc. IEEE Ultrasonics Symp., October 1977, pp. 877-881.
22. J.A. Kusters and J.G. Leach, "Further Experimental Data on Stress and Thermal Gradient Compensated Crystals", Proc. IEEE, Vol. 65, February 1977, pp. 282-284.
23. A. Ballato, "Doubly Rotated Thickness Mode Plate Vibrators", in Physical Acoustics: Principles and Methods, (W.P. Mason and R.N. Thurston, eds.), Vol. 13, Chap. 5. Academic Press, New York, 1977, pp. 115-181.
24. T.J. Young, D.R. Koehler, and R.A. Adams, "Radiation Induced Frequency and Resistance Changes in Electrolyzed High Purity Quartz Resonators", Proc. 32nd AFCS, May-June 1978, pp. 34-42.
25. J.A. Kusters, M.C. Fischer, and J.G. Leach, "Dual Mode Operation of Temperature and Stress Compensated Crystals", Proc. 32nd AFCS, May-June 1978, pp. 389-397.
26. F. Euler, P. Ligor, A. Kahan, P. Pellegrini, T.M. Flanagan, and T.F. Wrobel, "Steady State Radiation Effects in Precision Quartz Resonators", Proc. 32nd AFCS, May-June 1978, pp. 24-33.
27. E.P. EerNisse, Sandia Laboratories, Albuquerque, NM 87185, private communication, June 1978.
28. R. Bechmann, "Frequency-Temperature-Angle Characteristics of AT-Type Resonators Made of Natural and Synthetic Quartz", Proc. IRE, Vol. 44, November 1956, pp. 1600-1607.
29. T. Parker, Raytheon Research Division, Waltham, MA 02154, private com-

munication, December 1978.

30. S.J. Hughes, Royal Aircraft Establishment, Farnborough, private communication, June 1978.
31. J. -J. Gagnepain, C.N.R.S., Besançon, private communication, November 1978.
32. G. Lagasse, McCoy Electronics Co., Mount Holly Springs, PA 17065, private communication, June 1978.
33. E.P. EerNisse, "Quartz Resonator Frequency Shifts Arising from Electrode Stress", Proc. 29th AFCS, May 1975, pp. 1-4.
34. E.P. EerNisse, "Calculations on the Stress Compensated (SC-cut) Quartz Resonator", Proc. 30th AFCS, June 1976, pp. 8-11.
35. E.P. EerNisse, "Rotated X-Cut Quartz Resonators for High Temperature Applications", Proc. 32nd AFCS, May-June 1978, pp. 255-259.
36. R.J. Besson, E.N.S.C.M.B., Besançon, and F.L. Walls, N.B.S., Boulder, CO 80303, Private communications, May 1978.
37. S.R. Stein, C.M. Manney, Jr., F.L. Walls, J.E. Gray and R.J. Besson, "A Systems Approach to High Performance Oscillators", Proc. 32nd AFCS, May-June 1978, pp. 527-530.
38. F.L. Walls and S. Stein, "A Frequency-Lock System for Improved Quartz Crystal Oscillator Performance", IEEE Trans. Instrum. Meas., Vol. IM-27, September 1978, pp. 249-252.

DEPARTMENT OF THE ARMY
HEADQUARTERS
UNITED STATES ARMY
ELECTRONICS RESEARCH & DEVELOPMENT COMMAND
FORT MONMOUTH, NEW JERSEY 07703
ATTN: ~~DELET-NM~~
OFFICIAL BUSINESS



POSTAGE AND FEES PAID
DEPARTMENT OF THE ARMY
DOD-314